Structural analysis of solar panel cleaning robotic arm

Amit Kumar Mondal and Kamal Bansal

The efficiency of solar photovoltaic (SPV) panels depends upon the amount of solar irradiance and spectral content. SPV panels are being widely used because of their economic and environmental merits. The performance of SPV panels gets degraded due to factors like air pollution, bird droppings, dust, snow accumulation, etc. An automatic and integrated solar panel cleaning robotic arm (SPCRA) with four-degrees of freedom has been designed to overcome the above factors. The arm has two prismatic and two revolute joints. SPCRA has a unique end effector with a water sprinkler, air blower and a wiper installed as a single unit on it. Few traits like anti-interloped design, automated grid cleaning mechanism, efficient algorithm, all-weather cleaning support, and plug-n-play strategy with optimum costs make it a versatile system for cleaning the SPV panels.

With the growing cost of energy and adverse effects of conventional fuels over the environment, implementation of green fuels like solar power is on demand. Solar power is mainly harnessed by solar photovoltaic (SPV) panels. Its efficiency degrades due to accumulation of dust and debris over SPV panels[1]. Table 1 gives an overview of the improvement in efficiencies using the current PV technologies. Dust is the most common factor which decreases the efficiency of such technologies. It acts as an obstruction for the incident light to reach the cells, causing reduced efficiency due to lower power output. Dust accumulation occurs at different rates in different parts of the world depending upon the local wind conditions[2], panel orientation[3] and nature of dust[4].

Different cleaning methods are currently being used both at industrial as well as domestic level. Labour-based cleaning method for SPV panels is costly, time-consuming and requires technical skill, which also leads to wastage of water and energy and lacks automation capabilities. Existing solutions are also dependent on geographical terrain and area of application. Depending on these factors, existing solutions can be further compared on the basis of cost, ease of use, performance rate, etc. These solutions are not universally applicable for all situations (Table 2). The existing solutions are not only limited to the Earth, but are being used in Mars as well.

Table 1. Efficiencies of different solar photovoltaic technologies

PV technology	Efficiency (%)
Carbon nanotubes (CNT)[19]	3–4
Amorphous silicon[20]	5–7
Poly crystalline silicon[21]	8–12
Dye-synthesized[22]	11.1
Mono crystalline silicon[23]	15–18
Other thin films (CdTe, CIS, etc.)[24,25]	16–20
Triple junction under concentrated Sun[26]	Up to 37.4
Hot carrier solar cell[27]	66

The developed solar panel cleaning robotic arm (SPCRA) is a robotic arm that can clean SPV panels. SPCRA is an ergonomically designed system with traits like anti-interloped design, automated grid cleaning mechanism, efficient algorithm, all-weather cleaning support, plug-n-play strategy and economical establishment costs. The system includes a guide rail that will be installed parallel to the pre-installed SPV panels. The anti-interloped design will prevent damage to the SPV panels in case of any adverse incident. The guide rails will support the base of the cleaning arm, which will be driven by a motor and controlled by ultrasonic/proximity sensors. The arm adjustment always ensures that the system is parallel to the cleaning surface. The inclination of the arm is controlled by the ultrasonic/proximity sensors installed at the specific pre-defined angle (depending on individual panels). The arm is made up of a hollow rectangular beam, so as to properly utilize the space of the robotic arm and to provide a dynamic balance. The motion of the cleaning head is controlled by the ultrasonic/proximity sensors installed at the upper and lower ends of the arm. Worm-geared DC servo motor and DC motors are used to control the direction and inclination of the robotic arm.

Configuration of SPCRA

Users of SPCRA

It is intended that users of SPCRA are the SPV installation companies, manufacturing companies and their end-users. The consumers having SPV-based power plants (installed in arrays) find it difficult to clean them with current methods as listed in Table 3.

Arrangements of SPCRA

SPCRA consists of a robotic arm, rail-guided system, chain sprocket assembly and end effector.

The four-degrees of freedom (DOF) robotic arm is powered with worm-geared 12 V DC servo motor and is mounted on a base, installed over a rail-guided platform. Base and rail-guided platform is coupled with a geared system which is powered with a side shaft 12 V DC geared motor. The chain sprocket assembly installed on the arm is powered by a side shaft 12 V DC geared motor with bidirectional encoder fitted on the assembly. Rail-guided system rolls over a T-beam made up of mild steel with the help of a gear mechanism attached with a side shaft 12 V DC geared motor. The end effector has water-sprinkler, air-blower and wiper. The end effector is attached to the chain sprocket system which slides on the arm.

To observe the whole process, camera surveillance has been provided using Logitech HD webcam[5]. The camera is kept at a distance which can cover the whole SPV panel arrays. The SPV panels can be cleaned periodically depending upon the information received from the camera.

Table 2. Comparison of cleaning systems[28]

Cleaning system	Advantage	Disadvantage
Solar panel cleaning robot[29]	Washing and wiping, both process are present.	Horizontal shifting of the robot over the PV module results in skidding. Weight of the robot is over the SPV module.
Gekko solar[30]	Self-regulating and flexible, uninterrupted cleaning operations.	Limitation of inclination up to 45°. Complex, vaccum-based, gear, belt system.
Gekko solar farm[31]	Self-regulating and flexible, uninterrupted cleaning operations.	Limitation of inclination up to 30°. Complex gear belt system.
Wash panel's solar panel cleaning robot[32]	Able to clean dust and bird droppings.	Human intervention is required to start the operation and while moving from one row to another.
Hector[33]	Compatible, integrated with all supplies. Operational day and night.	Performance is slow. Feeding has to be done regularly
Solar brush[34]	Automated robot. Works up to an inclination of 35°. Wireless controlled. Rechargeable.	Heavy weight. Initial cost is high. Requires human intervention. Performance speed is very slow.
PIC microcontroller[35] and PLC-based cleaning[36]	Self-regulating and flexible, uninterrupted cleaning operations.	Complex chain, sprocket-based structure. Single-panel-based design.
Heliotex's 'Automatic solar panel cleaning system'[37]	Water reaches to every part of the SPV modules. Helps in cooling of SPV modules, which increases the efficiency.	Treated water required. Filter has to be change periodically. Huge wastage of water.
Tuff Fab's nano clear[38]	Long-lasting.	Cleaning is still required, but with less effort.
EDS for standing-wave electric curtain[39]	Highly efficient at high gas pressure. No mechanical movement to scratch the protective surface.	Removal is difficult when gas (atmospheric) pressure is below a certain limit. Dust removal capability depends on the size of the particles deposited. Requires high voltage.
EDS for multiphase electric curtain[40–42]	Efficient and can be used to remove dust from a variety of surfaces. No mechanical movement to scratch the protective surface. Efficient with and without use of external power supply.	Requires Digital Signal Controller, which is costly. Requires switching devices for converters, hence more maintenance is required. Requires high voltage.
Greenbotic's GB1[43]	Able to clean dust and bird droppings.	Human intervention is required to start the operation and while moving from one row to another.

Mechanical design of SPCRA

In the design of the SPCRA, many factors are considered such as weight, assembly and disassembly of parts, workspace, load capacity, speed, repeatability and accuracy, volume, energy, efficiency and cost[6]. Rigid-link manipulators require light, stiff structures to achieve high accuracy and low inertia. While designing the manipulator various factors were taken into consideration. These included DOF of end factor[7], path constraints and motion solution[8], placement, design and aesthetics of the robot[9], material required to withstand all the forces and structural stability[10]. The design parameters such as size of end effector[11] and the working mechanisms[12] were also taken into consideration. Analysis of stiffness[8,13], and displacement of manipulator links has been done with the help of solid works. Optimization[13] and calibration techniques[14] have been used to correct errors in accuracy. While designing manipulator arm, light

Table 3. Characteristic features of different methods of cleaning

Methods	Features
Water sprinkler	Excessive loss of water. Spreading of water/reach is not uniform. Economically not viable for SPV plants.
Human effort	Costly as person has to be a technically trained. Reach is not uniform.
Existing cleaning modules available (like Clean Anti Prof, Cleaning Ant Junior, Gekko Junior G4, etc.)	Cleaning robot weight is directly put over the SPV panels. Power consumption is more. Performance area is less.
Proposed robotic arm	Minimum consumption of water. Power consumption is less. Performance area is more.

weight material[15] with high strength was chosen.

The robotic arm has four DOF, it comprises of two revolute and two prismatic joints. Design of the robotic arm should focus on its weight. Designed end effector weight is 500 g, which includes weight of cleaning head mechanism. The length of the robotic arm is 1.4 m. The robotic arm is connected with the worm-geared 12 V DC servo motor placed at the bottom of the link in the base. The advantage of the worm gear assembly is: (i) right angle power transmission and (ii) no need of stall torque, worm gear arrangement will hold the load during no power.

Hence, the robotic arm consumes less power and SPV panels are protected from any mishap. The material of the arm is chosen as aluminium (AI6063; Grade T5) for light weight and high strength. The chain sprocket assembly from Vex Robotics[16] is made up of reinforced material and can transmit heavy loads up to 22.6 kg over long distances. To move this chain sprocket assembly side shaft geared DC motor (85 rpm)[17] with bi-directional encoder is fitted having a stall torque of 21 kg/cm @ 12 V. The base holds the arm with the help of worm geared 12 V DC servo motor placed at the bottom of the link. It also holds few other parts of the robotic assembly like blower, mini water tank with pump, and side-shaft DC motor coupled with the guide rail. Because of the other components placed on it, the counterweight tilts while the robotic arm is tilted towards the SPV panels. To make the base area small and with high strength, we made it circular and the material used was mild steel.

The rail-guided platform is made up of mild steel. It carries the whole structure of the robot, which includes arm and base (and its components, shown in Figure 1). Considering the gross weight of the robot, material strength and ease of fabrication, mild steel is selected for the rail-guided platform. Complete robot is moved with the help of a 12 V side shaft DC motor, which is coupled with the T-beam rail (made up of cast iron) using gear mechanism. Structural analysis shows that it is the major load-bearing component and hence has to be structurally sound and stable. The base of the arm (along with gear system and other parts) and the arm itself are kept on top of it, which exerts a combined load of few kilo Newton of force. The self weight of the structure is also considered in the analysis. The structure is made purely out of mild steel, except the arm which is made from aluminium. The mechanical properties of the selected materials are given Table 4.

The types of load exerted on this component include: (i) normal load due to the base and the arm arrangement; (ii) a torque applied to at a distance by the gear arrangement and (iii) self-weight of the component.

Stress, strain and displacement are analysed using the software solidworks.

The results of the structural stability analysis of SPCRA are in Table 5. This analysis indicates that we need to release the stress from the specified location. It can be done either by heat treating the component to bring it to a specified strength or using the same material for welding as the base material to maintain the uniformity of the properties.

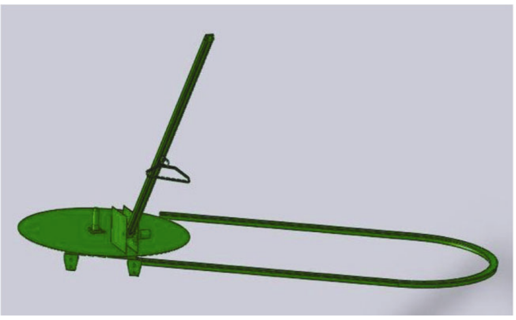

Figure 1. Complete overview of the SPCRA system.

Table 4. Mechanical properties of cast iron and aluminium (Arm)-6063-T5

Property	Iron	Aluminium
Elastic modulus	6.61781×10^{10} N/m^2	6.9×10^{10} N/m^2
Shear modulus	5×10^{10} N/m^2	2.58×10^{10} N/m^2
Density	7200 kg/m^3	2700 kg/m^3
Tensile strength	1.51658×10^8 N/m^2	1.45×10^8 N/m^2
Compressive strength	5.72165×10^8 N/m^2	5.72165×10^8 N/m^2

Basic tasks of SPCRA

Figure 2 shows the basic tasks of SPCRA. The working of SPCRA is as follows:

- Initially SPCRA will come to its home position P0 shown in Figure 2.
- From its home position it will go to its position P1, which will be determined using an ultrasonic sensor[18] kept in one of the ends of SPCRA's rail-guided system. These positions are prior marked via mild steel rods kept at a proper distance in proportion to the cleaning length (wiper length).
- On reaching its first position, the guide rail system will stop and the arm will start tilting towards the SPV panels. When the arm becomes parallel (adjusted during the fitting/construction) to the SPV panel, it stops and now the cleaning head comes into play.

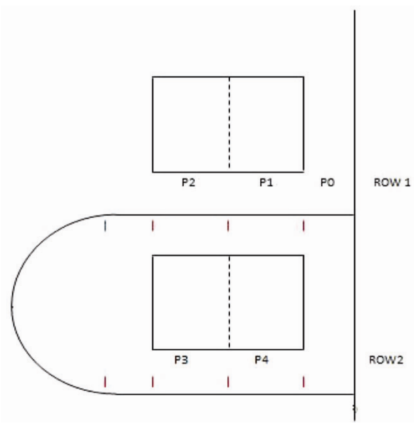

Figure 2. SPCRA testing field. P0: Home condition; P1, P2: Positions 1 and 2 of SPV panel 1; P3, P4: Positions 3 and 4 of SPV panel 2; Red, blue lines are halt points of SPCRA.

- Cleaning head starts from the top of the inclined SPV panel to its base, where it stops. The cleaning area (from top to bottom of SPV) is decided using ultrasonic sensors which are placed on the top and the bottom of SPCRA's arm.
- Now the arm lifts itself a few degrees up and during this time simultaneously the cleaning head goes up. By this, position 1 is cleaned and now SPCRA moves to position 2.
- After cleaning of row 1, SPCRA comes out and enters the semi-curricular path where it stops in between and rotates 180° and proceeds further.
- On reaching, beginning of row 2, the entire above-mentioned process is repeated.

Figure 3 shows the SPCRA model with labelling.

Results

The PV system has an installed capacity of base 100 kW, which consists of two modules. It was installed on a flat concrete base in the ground. The SPV modules were thin-film silicon wafers with anti-reflective coatings to maximize sunlight absorption. The modules were installed at an angle of 29.8°C (≈ 30°C). The set-up was installed using metal frames. One SPV was left (uncleaned (periodically) throughout the monitoring period and the other was cleaned excess time before taking the reading; this was done to mimic and compare the actual scenario. As the comparison is based on the efficiency enhancement and short-circuit current difference, one of the SPV modules was kept uncleaned and the other cleaned. During this process both the SPV modules were kept under similar conditions like solar radiation, surface temperature, etc. After a fixed interval of six days, the uncleaned panel was cleaned using SPCRA.

Monitoring results

Monitoring of the test rig, data collection, performance analysis and reporting were done. Data were collected for a period of four weeks from 1000 to 1700 h

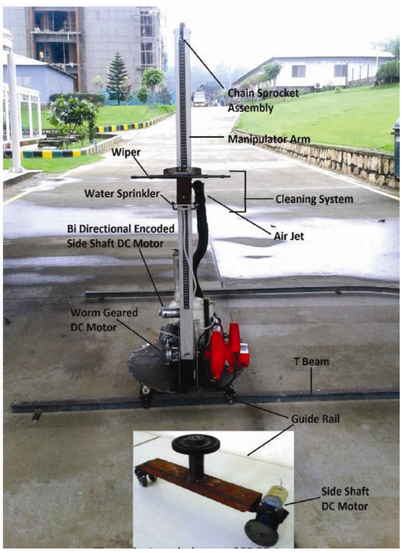

Figure 3. Actual photograph of SPCRA.

Table 5. Structural stability analysis of SPCRA

Part	Property	Values	
		Minimum	Maximum
Rail guided system	Displacement (mm)	10^{-30}	3.7×10^{-4}
	Stress	0	4.53×10^{-7}
	Strain	0	0.2
Circular base	Displacement (m)	1.72×10^{-4}	10^{-33}
	Stress	102.5	710450.8
	Strain	0	0.748
Arm	Displacement (mm)	10^{-30}	0.3654
	Stress (N/m^2)	696	6,389,769
	Strain	7.4×10^{-9}	6.9×10^{-5}

Table 6. SPV specifications

PV module/array	Specification
Type	Thin film solar module (double junction a-Si)
Application class	Class A
Nominal P_m	50 W
Maximum system voltage (V_{sm})	1000 V
Open circuit voltage (V_{oc})	62 V
Short circuit current (I_{sc})	1.42 A
Dimension	1245 × 635 × 7.5 mm

Table 7. Weekly power loss due to natural soiling depending on ambient conditions

Days	Week 1	Week 2	Week 3	Week 4
1	–17.3567	20.0256	3.4166	–28.6655
2	–5.95497	14.23332	0.23062	49.50207
3	–3.97074	4.05834	12.62366	4.67615
4	29.37738	25.29583	8.8253	25.08953
5	20.15533	12.37975	14.78451	24.89871
6	27.76095	17.34945	21.72536	51.53253

Table 8. Energy consumption of SPCRA for one-time cleaning

Action	Average current (A)	No. of cycles	Total time consumed (sec)	Energy consumed (mAh)
SPCRA platform motion on guide rail	0.385	3	18	5.775
ARM motion (rotatory)	0.65	6	8.25	8.9375
Base platform rotation	0.41	1	6	0.6833
Cleaning head	0.39	12	24	31.2
Total				46.5958

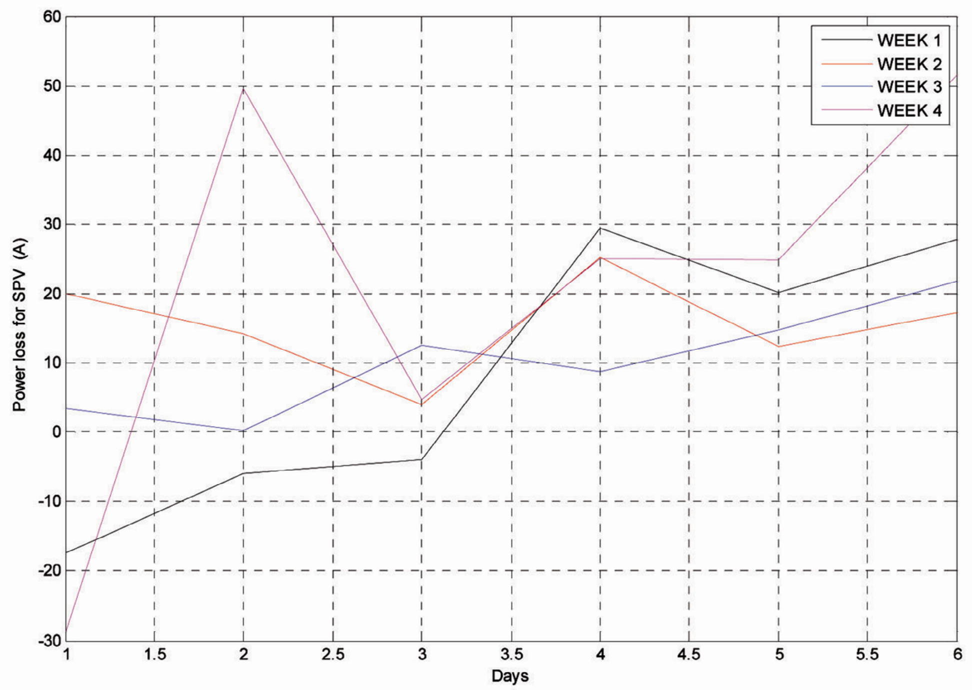

Figure 4. Weekly power loss due to natural soiling under ambient conditions.

over an interval of 30 min (SPV specifications are given in Table 6). Data were monitored for both the SPV modules (cleaned and uncleaned), and the following observations were made:

(i) Short circuit current (I_{sc}): Drop in I_{sc} due to soiling, was observed over the period for a week.
(ii) Energy yield: The effective loss in terms of power is shown in Table 7. As the dust accumulation increases, the power loss is highest on the last day of the week, compared to first day, which has been shown in Figure 4.
(iii) SPV Module Temperature: Day wise variation of SPV module surface temperature and short circuit current, I_{sc}.

From Table 8, the power consumption for cleaning a single SPV is 35.708 W using SPCRA. Considering the peak sunshine condition at 1100 h on 14 November 2014, open circuit voltage (V_{oc}) and I_{sc} values for both the panels were taken and compared. V_{oc_1} = 54.06 V, I_{sc1} = 1.147 A, and P_1 = 62.00682 W, V_{oc_2} = 54.03 V, I_{sc_1} = 1.042 A and P_2 = 56.29926 W.

Amount of power loss due to natural soiling for a particular instant of a day = 8.95661 W.

Considering the above value for a week = 63 W.

Amount of energy saving for a single SPV module = 63 – 35.708 = 27.292 W.

% Enhancement in efficiency = 9.1%.

Conclusion

We have discussed the cleaning technology using an electromechanical system for SPV. The system has been analysed and optimized for high effectivity. The external system developed does not affect the actual performance of SPV, since it is not coupled with the panels.

As the tests were conducted on 50 W SPV panels, the efficiency enhancement value is less. If the same tests were conducted over SPV modules of higher wattage rating (keeping the same surface area), then the efficiency enhancement would have been a much better significant value.

1. Ibrahim, A., *J. Basic Appl. Sci. Res.*, 2011, **1**(3), 222–230.
2. Goossens, D., Offer, Z. Y. and Zangvil, A., *Sol. Energy*, 1993, **50**, 75–84.
3. Smits, K. and Goossens, D., *Appl. Sol. Energy*, 1995, **30**, 75–89.
4. El-Shobokshy, M. S. and Hussein, F. M., *Renew. Energy*, 1993, **3**, 585–590.
5. http://www.logitech.com/en-us/product/hd-webcam-c525
6. Song, W. K., Lee, H. and Bien, Z., *Robotics Autonomous Syst.*, 1999, 83–94.
7. Rivin, E. I., Holbrook, R., Bhatt, S. and Bhattacharya, A., *ASME: Dyn. Syst. Control*, 1987, **6**, 253–259.
8. Kakizaki, T., *Jpn. Soc. Mech. Eng.*, 1991, **57**, 1961–1968.
9. Nof, Y. S., *Handbook of Industrial Robotics*, John Wiley, New York, 1985.
10. Khurmi, R. S., *A Textbook of Machine Design*, S. Chand and Co Ltd, 2005.
11. Rivin, E., *Mechanical Design of Robots*, McGraw-Hill, 1988.
12. Andeen, G. B., *Robot Design Handbook*, McGraw-Hill, New York, 1988.
13. Leu, M. C., Dukovski, V. and Wang, K., In Proceedings of Symposium Robotics Manufacturing Automation, 1985, pp. 137–143.
14. Roth, Z. S., Mooring, B. and Ravani, B., *Robotics Automation*, 1987, **3**(5), 377–385.
15. Priebe, H. M. J. and Paul, C., *Robotics Automation*, 1987.
16. http://ieeexplore.ieee.org/xpl/freeabs_all.jsp?arnumber=1087976; http://www.vexrobotics.com/276-2252.html
17. http://www.nexrobotics.com/product-stopmenu45.html?page=shop.product_details&flypage=flypage.tpl&product_id=877
18. http://www.rhydolabz.com/index.php?main_page=product_info&products_id=307
19. http://www.news.cornell.edu/stories/sept-09/NanotubeSolarCells.html

20. Parida, B., Iniyan, S. and Goic, R., *Renew. Sustain. Energy Rev.*, 2011, **15**, 1625–1636.
21. Becker, C., Sontheimer, T., Steffens, S., Scherf, S. and Rech, B., *Energy Proc.*, 2011, **10**, 61–65.
22. http://en.wikipedia.org/wiki/Solar_cell
23. Razykov, T. M., Ferekides, C., Morel, D., Stefanakos, E., Ullal, H. and Upadhyaya, H., *Sol. Energy*, 2011, **85**, 1580–1608.
24. Morales-Acevedo, A., *Sol. Energy*, 2006, **80**, 675–681.
25. Barnett, A. M. *et al.*, *Sol. Energy Mater. Solar Cells*, 2001, **66**, 45–50.
26. Yamaguchi, T., Takamoto, T. and Araki, K., *Sol. Energy Mater. Solar Cells*, 2006, **90**, 3068–3077.
27. Ross, R. T. and Nozik, A., *Appl. Phys.*, 1982, **53**, 3813–3818.
28. Lamont, L. A. and Chaar, L. E., *Renew. Energy*, 2011, **36**, 1306–1310.
29. Anderson, M., Grandy, A., Hastie, J. and Sweezey, A.,
30. http://serbot.ch/images/documents/TD_GEKKO%20Solar_En_2013_06_06.pdf
31. http://serbot.ch/images/documents/TD_GEKKO%20Solar%20Farm_En_2013_06_26.pdf
32. http://www.washpanel.com/en/documenti.php
33. http://www.seneraerospace.com/AERO-ESPACIAL/ProjectsD/hector-cleaning-robot-system-for-heliostats/en
34. http://www.solarbrush.de/about
35. Al-Qubaisi, E. M., Al-Ameri, M., Al-Obaidi, A., Rabia, M., Chaar, E. and Lamont, L., In International Conference on Electric Power and Energy Conversion Systems, 2009.
36. Dhaheri, A., Lamont, L., Chaar, E. L. and Al-Ameri, O., In International Conference on Transmission and Distribution Conference and Exposition, New Orleans, LA, USA, 2010.
37. http://www.solarpanelcleaningsystems.com/solar-panel-cleaningservices.php
38. http://www.tufffab.com/solar-panel-glass-coatingsolution.html
39. Atten, P., Pang, H. and Rebound, J., *IEEE Trans. Ind. Appl.*, 2009, **45**(1), 75–86.
40. Mazumder, M. K., Sims, R. A. and Wilson, J. D., AR (US) Patent US 6911593, 2005.
41. Bock, J. P., Robinson, J. R., Sharma, R., Zhang, J. and Mazumder, M. K., In ESA Annual Meeting on Electrostatics, 2008.
42. Melcher, J. R., Warren, E. and Kotwal, R., *IEEE Trans. Ind. Appl.*, 1989, **25**(5), 956–961.
43. http://www.greenbotics.com/projects.html

ACKNOWLEDGEMENTS. We thank Mukul Gupta and G. G. Sastry (University of Petroleum and Energy Studies, Dehradun) for support and encouragement.

Received 25 July 2014; revised accepted 15 December 2014

Amit Kumar Mondal is in the Electronics and Instrumentation Department, and Kamal Bansal in the Electrical, Power and Energy Department, University of Petroleum and Energy Studies, Dehradun 248 007, India.*
**e-mail: akmondal1603@gmail.com*